

Synthesis, Characterization, DNA Binding Properties, Fluorescence Studies and Toxic Activity of Cobalt(III) and Ruthenium(II) Polypyridyl Complexes

Penumaka Nagababu · Mynam Shilpa · J. Naveena Lavanya Latha · Ira Bhatnagar ·
P. N. B. S. Srinivas · Yata Praveen Kumar · Kotha Laxma Reddy ·
Sirasani Satyanarayana

Received: 27 May 2010 / Accepted: 29 September 2010 / Published online: 8 October 2010
© Springer Science+Business Media, LLC 2010

Abstract The new ligand 4-(isopropylbenzaldehyde)imidazo[4,5-*f*][1,10]phenanthroline (ippip) and its complexes [Ru(phen)₂(ippip)]²⁺ (**1**), [Co(phen)₂(ippip)]³⁺ (**2**), [Ru(bpy)₂(ippip)]²⁺ (**3**), [Co(bpy)₂(ippip)]³⁺ (**4**) (bpy=2,2-bipyridine) and (phen=1,10-phenanthroline) were synthesized and characterized by ES⁺-MS, ¹H and ¹³C NMR. The DNA binding properties of the four complexes were investigated by different spectrophotometric methods and viscosity measurements. The results suggest that complexes bind to calf thymus DNA (CT-DNA) through intercalation. When irradiated at 365 nm, the complexes promote the photocleavage of pBR322 DNA, and complex 1 cleaves DNA more effectively than 2, 3, 4 complexes under comparable experimental conditions. Furthermore, photocleavage studies reveal that singlet oxygen (¹O₂) plays a significant role in the photocleavage.

Keywords Cobalt(III) and ruthenium(II) mixed-ligands · DNA-binding · Fluorescence studies · Photocleavage of plasmid DNA · Toxic studies

Introduction

Among the host of DNA-binding and cleaving agents reported so far, transition metal complexes are of relevance to the present work. Major interests in this regard concern the utility of metal complexes in the development of site specific cleavers, structural/spectroscopic probes, restriction enzymes, molecular photo switches and, of course, anti-tumor drugs. Metal complexes have been found to be particularly useful for the above mentioned purposes because of their potential to bind DNA through multitude of interactions and to cleave the duplex by virtue of their intrinsic chemical, electrochemical and photochemical reactivities. During the last decade, a number of transition-metal complexes have been utilized to probe nucleic acid structure [1, 2], and in the development of DNA-cleaving agents [3, 4], DNA photo probes [5, 6] DNA-molecular light switches [7, 8] and so forth. It has also been well documented that metal complexes can bind to DNA covalently as well non covalently [6, 9].

On the other hand, Barton and co-workers reported that a number of metal complexes containing aromatic diimine ligands [10] could act as photoluminescent metal-based probes for the study of DNA binding. These complexes have been reported to bind DNA through π - π^* and/or electrostatic interactions and cause oxidative cleavage of DNA. Moreover, an oxidative cleavage of DNA on irradiation with visible light has gained considerable interest due to its potential application in photodynamic

P. Nagababu · M. Shilpa · Y. P. Kumar · K. L. Reddy ·
S. Satyanarayana (✉)
Department of Chemistry, Osmania University,
Hyderabad, Andhra Pradesh, India PIN-500 007
e-mail: ssnisirasani@gmail.com

I. Bhatnagar
CCMB (Centre for Cellular and Molecular Biology),
Hyderabad 500007, India

P. N. B. S. Srinivas
National Institute of Nutrition,
Hyderabad, India

J. N. L. Latha
Department of Biotechnology, Krishna University,
Machilipatnam, India

therapy of cancer [11, 12]. Recently, several mixed ligand complexes of ruthenium(II) and cobalt(III) have also been reported [13–16]. In view of the above, we explore DNA binding and photo-induced cleavage activity of cobalt and ruthenium complexes.

Experimental

Materials

CT (calf thymus) DNA was purchased from Aldrich. The synthesis of 1,10 phenanthroline-5, 6-dione was prepared as per the procedure given in literature [17]. Interactions of the complexes with DNA were studied in tris buffer (5 mM Tris-HCl, 5 mM NaCl, p^H 7.0). DNA had a ratio of UV absorbance at 260 and 280 nm of about 1.90 indicating its purity [18]. The DNA concentration per nucleotide was determined by absorbance at 260 nm using the molar absorption coefficient ($6,600 \text{ M}^{-1} \text{ cm}^{-1}$) [19].

Synthesis of Ligands

(ippip) = 4-(isopropyl benzaldehyde)imidazo[4,5-*f*][1, 10] phenanthroline

Phen-dione (0.53 g, 2.50 mmol), 4-isopropyl benzaldehyde (0.152 g, 1.2 mmol) and ammonium acetate (3.88 g, 50.00 mmol) and glacial acetic acid (15 mL) were refluxed together for 4 h as per Steck and Day [20], cooled thereafter to room temperature and diluted with water. Dropwise addition of liquor ammonia gave a yellow precipitate which was collected, washed with water, dried and purified by recrystallization. Formula: $\text{C}_{22}\text{H}_{18}\text{N}_4$, Anal. Calc. H 5.36, C 78.08, N 16.56 found: H 4.9, C 77.0, N 15.6 (yield=80%) Analytical data: ES^+ -MS calculated: 338.15 found: 339. ^1H NMR (DMSO, TMS): 9.03 (d, 2H), 8.95 (d, 2H), 8.24 (d, 2H), 7.21 (d, 1H), 7.03 (d, 1H), 6.95 (d, 1H), 2.51(d, 1H), 1.65 CH_3 peak.

Synthesis of Complexes

[Ru(phen)₂(ippip)](ClO₄)₂ · 3.5H₂O

A mixture of $[\text{Ru}(\text{phen})_2\text{Cl}_2] \cdot 2\text{H}_2\text{O}$ (0.531 g, 1.0 mmol), ippip (0.489 g, 1.0 mmol) and ethanol (15 mL) was thoroughly deoxygenated. The purple mixture was heated for 8 h at 120 °C under N_2 atmosphere. When the solution finally turned red, it was cooled to room temperature and an equal volume of saturated aqueous sodium perchlorate solution was added under vigorous stirring. The red solid was collected and washed with small amounts of water, ethanol, and diethyl ether, then dried under vacuum, (yield=

60%). Analytical data for $\text{RuC}_{46}\text{H}_{39}\text{N}_8\text{Cl}_2\text{O}_{12}$. ES^+ -MS cal: 1,060 found: 1,059. IR: 1,479 (C=C), 1,598 (C=N), 721 (Co–N (L)), 623 cm^{-1} (Co–N(ippip)). ^1H NMR (DMSO, TMS): 9.09 (d, 6 H), 8.74 (d, 6 H), 8.50 (d, 4H), 8.28 (s, 4H), 8.13 (t, 4H), 8.02(t, 2H), 7.99 (d, 2H), 7.53 (d, 1H), 7.35(d, 1H), 3.61 (d, 1H), 1.8 CH_3 peak. ^{13}C NMR (200 MHz, DMSO, 298 K, major peaks) δ : 155.71, 155.38, 151.56, 151.30, 143.61, 143.42, 131.34, 127.32, 127.07, 126.87, 33.44, 23.64.

[Co(phen)₂(ippip)](ClO₄)₃ · 4H₂O

A mixture of $[\text{Co}(\text{phen})_2\text{Br}_2]\text{Br} \cdot 3\text{H}_2\text{O}$ (0.531 g, 1.0 mmol), ippip (0.489 g, 1.5 mmol) in ethanol (20 cm^3) was refluxed for 4 h to give a yellow solution. After filtration, the complex was precipitated by addition of a saturated ethanolic solution of NaClO_4 . The complex was filtered and further dried under vacuum before recrystallization ($\text{Me}_2\text{CO}-\text{Et}_2\text{O}$). (Yield=75%) Analytical data for $\text{CoC}_{45}\text{H}_{38}\text{N}_8\text{Cl}_3\text{O}_{16}$. ES^+ -MS calc:1,128 found:1,126. IR: 1,541 (C=C), 1,430 (C=N), 714 (Co–N (L)), 624 cm^{-1} (Co–N(ippip)). ^1H NMR (DMSO, TMS): δ 9.58(d, 6 H), 9.43(d, 6 H), 8.76 (d, 4H), 8.59 (s, 4H), 8.34 (t, 4H), 7.9(t, 2H), 7.74 (d, 2H), 7.55,(d,1H), 7.20,(d,1H), 3.8(d,1H), 1.6 CH_3 peak.

[Ru(bpy)₂(ippip)](ClO₄)₂ · 3 H₂O

This complex was synthesized as described above complex, (yield=63%), analytical data for $\text{RuC}_{42}\text{H}_{34}\text{N}_8\text{Cl}_2\text{O}_{11}$. ES^+ -MS calc: 1,004 found: 1,002. IR: 1,601 (C=C), 1,448 (C=N), 724 (Co–N (L)), 626 cm^{-1} (Co–N(ippip)). ^1H NMR ((DMSO, TMS), 300 MHz, TMS):

8.34 (d, 2H), 8.23(t, 2H), 8.16 (d, 2H), 8.10 (t, 3H), 8.0 (d, 2H), 7.971(m, 2H), 7.97(q, 4H), 7.93(d, 2H) 7.85(d, 2H), 7.7471(d, 2H), 7.5(d, 2H), 7.4(d, 1H), 7.34(d, 1H), 3.01(d, 1H), 1.5 CH_3 peak. ^{13}C NMR (200 MHz, DMSO, 298 K, major peaks) δ :152.87, 152.69, 150.91, 150.91, 150.165, 147.30, 147.22, 145.37, 136.86, 130.51, 128.13, 127.16, 126.75, 126.40, 126.10, 33.47, 23.77.

[Co(bpy)₂(ippip)](ClO₄)₃ · 2H₂O

This complex was synthesized as described above complex, with a mixture of $[\text{Co}(\text{bpy})_2\text{Br}_2]\text{Br} \cdot 3\text{H}_2\text{O}$ and ippip (0.564 g, 1.42 mmol), (yield=60%), analytical data for $\text{CoC}_{42}\text{H}_{34}\text{N}_8\text{Cl}_3\text{O}_{14}$. ES^+ -MS cal: 1,042 found: 1,040. IR: 1,560 (C=C), 1,448 (C=N), 718 (Co–N (L)), 622 cm^{-1} (Co–N(ippip)). ^1H NMR, (DMSO, TMS): δ 9.46(d, 2H), 9.44(d, 4H), 9.40(d, 2H), 9.1(m,4H), 8.72(d, 2H), 8.62(t, 4H), 8.42 (t, 2H), 8.15(m, 4H), 7.65(d, 2H), 7.5(d, 1H), 7.38(d, 1H), 3.1(d, 1H), 1.5 CH_3 peak. (Molecular structure of complexes Fig. 1).

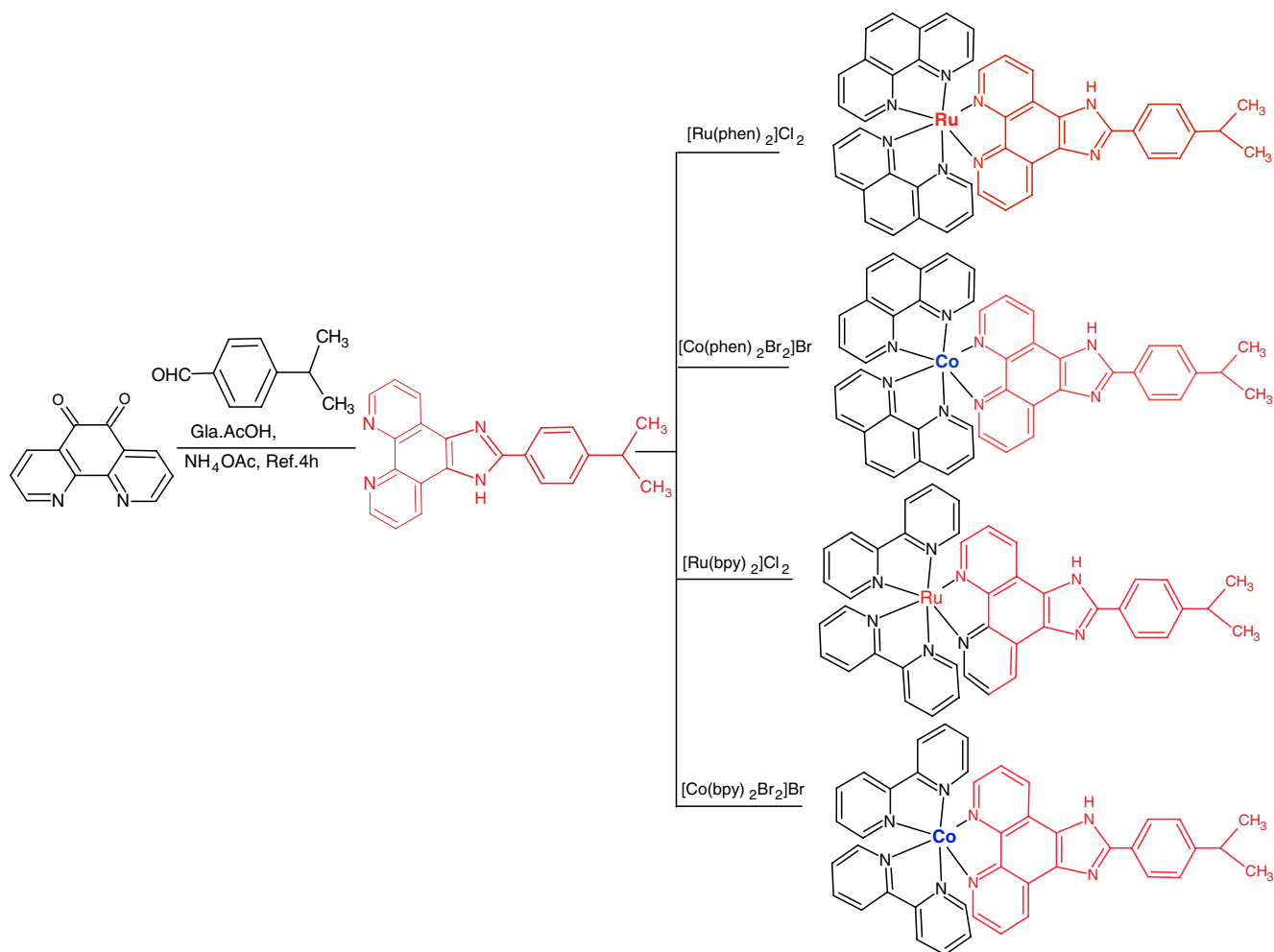


Fig. 1 Molecular structure of complexes

Physical Measurements

UV-Visible spectra were recorded in an *Elico Bio-spectrophotometer* model *BL198*. IR spectra were obtained in KBr phase in a *Perkin-Elmer FTIR-1605* spectrophotometer. NMR spectra were measured with a *Varian XL-400* MHz spectrometer with DMSO as solvent at room temperature and TMS as the internal standard. ES⁺-MS mass spectra were recorded. Microanalyses (C, H, N) were carried out with a *Perkin-Elmer 240* elemental analyzer. Fluorescence measurements were performed in a *HitachiF 4500* spectrofluorimeter.

Spectrophotometric titrations were carried out at room temperature to determine the binding affinity of complexes to DNA. For this, the reference cuvette contained tris-buffer (pH 7.0, 3.0 ml). The complex (30 μM in buffer, 3.0 ml) was taken in another sample cuvette. Spectra were recorded in the range of 200–600 nm. During the titration small aliquots of buffered DNA (1–10 μl, ~5 to 10 mM in NP) were added to both solutions mixed for ~5 min and then the

spectra were recorded. Titration was continued as above till there was no further change in absorption indicating saturation of binding. Change in concentration of complex due to dilution was negligible in view of the small volumes of DNA solution added. The above procedure was repeated minimum of three times.

Fluorescence emission titration experiments were performed at a fixed metal complex concentration (10 μM) to which DNA (1–160 μM) was added in a volume of (10–100 μL). Excitation wavelength was kept constant, emission was recorded. Fluorescence emission enhancement was based on comparison of emission intensity at 558 nm of complexes in the absence and presence of CT DNA.

Dialysis experiment were conducted at room temperature with 3 cm³ of CT-DNA (120 μM) sealed in a dialysis bag and 6 cm³ of complexes (20 μM) outside the bag with the solution stirring for 24 h.

Viscosity was determined in an Ostwald viscometer at 30.0±0.1° in a thermostated water-bath. CT DNA (~200 base pairs) was prepared by sonication [21]. Data are

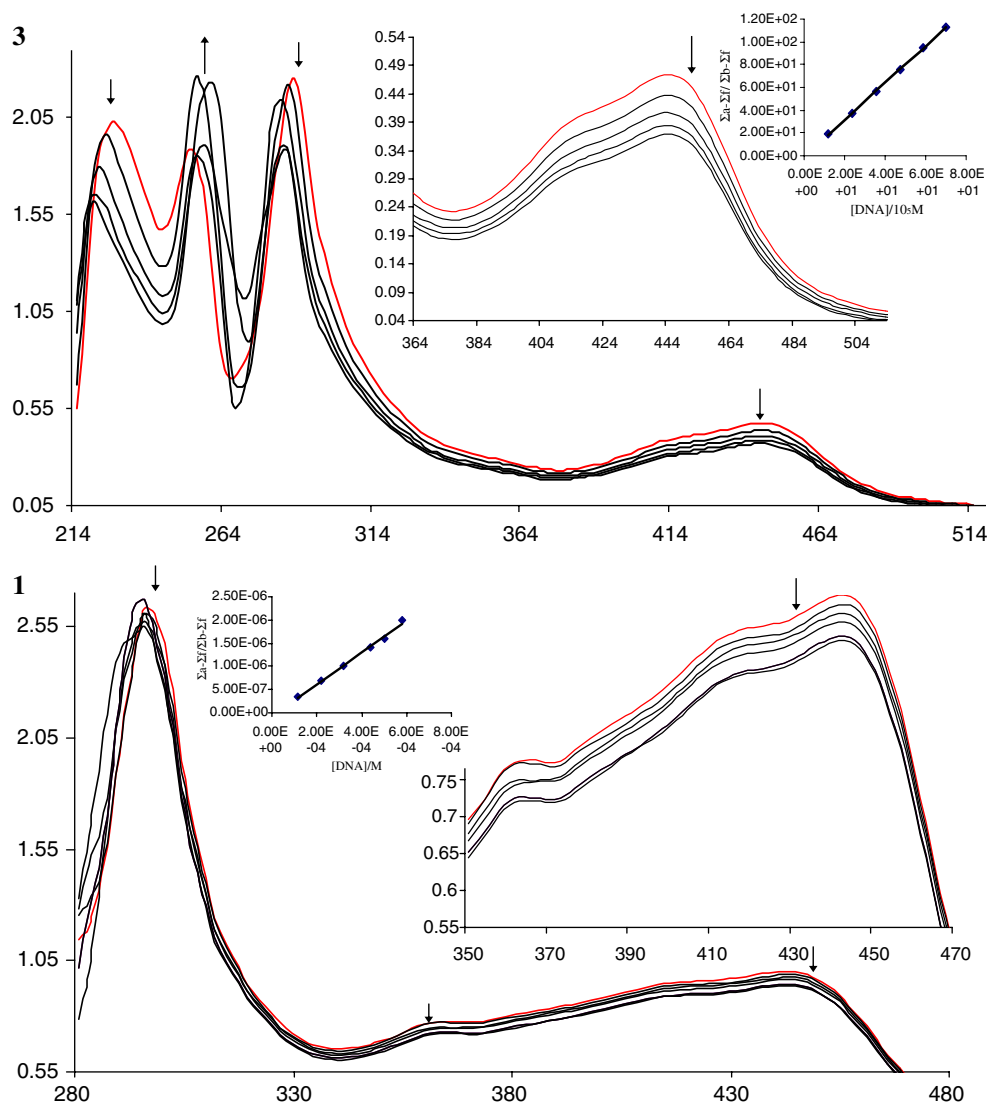
Table 1 Absorption spectrophotometric titration and thermal denaturation of DNA bound to complexes 1–4

Complexes	Excitation peaks	Emission peaks	UV/Vis peaks (nm)	$\Delta\lambda$	Absorption λ_{\max} (nm)		TM °C	Hypochromism (%)
					Free	Bound		
DNA alone	–	–	260 nm	–	–	–	60	–
1	274, 329, 383 nm	319, 358, 582 nm	298, 366, 446 nm	4	366	370	67	20%
2	358, 403, 451 nm	380, 359, 409 nm	297, 349 nm	3	297	300	66	19%
3	268, 318, 405 nm	360, 410, 591 nm	256, 288, 446 nm	3	446	449	64	17%
4	356, 452, 405 nm	370, 360, 409 nm	362, 302 nm	3	307	310	64	15%

presented as $(\eta/\eta_0)^{1/3}$ vs the concentration of complex bound to DNA, where η is the viscosity of DNA in the presence of complex and η_0 is the viscosity of DNA alone. Viscosity values were based on flow time of DNA-containing solution ($t > 100$ s) corrected for flow time of buffer alone (t_0), $\eta = t - t_0 / t_0$ [22].

Thermal denaturation studies were carried out with an *Elico Bio*-spectrophotometer model *BL198*, equipped with temperature-controlling programmer (± 0.1 °C). The absorbance at 260 nm was continuously monitored for solutions of CT-DNA (100 μ M) in tris-buffer in the absence and presence of the complex (10 μ M), with temperature

Fig. 2 Absorption spectra of complexes **3** and **1** in absence (red) and presence (lower) of DNA. [complex]=10 μ M; [DNA]/[complex]=0, 5, 10, 15. Arrow shows the absorbance changes upon increasing DNA concentrations. Insert plots of $[\text{DNA}]/[\varepsilon_a - \varepsilon_f]$ vs $[\text{DNA}]$ for the titration of DNA with complexes; (•) experimental data points; solid lines, linear fitting of the data



increments of 1 °C, min⁻¹. Supercoiled pBR322 DNA and complex mixture was irradiated for 1 h at $\lambda_{\text{max}}=365$ nm. All samples were analyzed by electrophoresis for 2.5 h at 40 v/cm on a 0.8% agarose gel in buffer, pH 8.2, gel DNA was visualized by staining with 1 $\mu\text{g/ml}$ ethidium bromide and then photographed under UV light.

The cell line HL-60 (human myeloid leukemia) was obtained from the National Centre for Cellular Sciences (NCCS), Pune, India. HL-60 cells were cultured in RPMI 1640 media supplemented with 10% (v/v) heat inactivated fetal bovine serum (FBS), 100 units/ml penicillin and 100 $\mu\text{g/ml}$ streptomycin. HL-60 cell lines were maintained in culture at 37 °C in an atmosphere of 5% CO₂.

Spectroscopic Characterization

The IR spectral data for the complexes exhibit bands at 1,458 cm⁻¹ and at 1,578–1,590 cm⁻¹ due to C=C and C=N vibrations of the ring respectively. Bands were present around 587 cm⁻¹ and 570 cm⁻¹ corresponding to Co–N (bpy) or Co–N of (phen). In the ¹H-NMR spectra of the complexes the peaks due to various protons of ligand shifted downfield compared to the free ligand suggesting complexation. As expected, the signal for the ligand appeared in the range around 7 to 9.8 ppm and the 6 hydrogens of the methyl group peaks appeared at 1.5–1.8 ppm

Results and Discussion

DNA-binding Studies

The absorption titrations of Ru(II) & Co(III) complexes in buffer were performed by using a fixed concentration of ruthenium or cobalt complexes concentration to which increments of the DNA stock solution (conc 4.5×10^{-4}) were added. Ruthenium (or) cobalt-DNA solutions were allowed to incubate for 5 min before the absorption spectra was recorded. The intrinsic binding constants K_b of complexes to DNA were derived as follows [23].

$$[\text{DNA}]/(\epsilon_a - \epsilon_f) = [\text{DNA}]/(\epsilon_b - \epsilon_f) + 1/(K_b(\epsilon_b - \epsilon_f))$$

where [DNA] is the concentration of CT-DNA in base pairs, the apparent absorption coefficients ϵ_a , ϵ_f , and ϵ_b correspond to $A_{\text{obsd}}/[\text{Ru}(\text{or})\text{Co}]$, the absorbance for the free complex, and the absorbance for the complex in fully bound form, respectively. K_b is given by the ratio of slope to intercept.

Absorption Titration

The absorption spectra of 1, 2, 3 and 4 complexes shows three or two well resolved bands in the range of 200–

600 nm. The bands below 300 nm are attributed to intraligand (IL) $\pi-\pi^*$ transitions, the band at 354 nm is attributed to the $\pi-\pi^*$ transition and the lowest energy bands at 446, 448, 349 and 362 nm for complexes 1, 2, 3 and 4 are assigned to the metal-to-ligand charge transfer (MLCT) transitions (Table 1) by comparison with the spectra of other polypyridyl Ru(II) complexes [24–27]. The application of electronic absorption spectroscopy in DNA-binding studies is one of the most useful techniques. The complex binding with DNA through intercalation usually results in hypochromism and bathochromism. The interaction of these complexes with CT-DNA was monitored by the absorption titration method. In the presence of increasing CT-DNA, both complexes 1, 3 showed a strong decrease in intensity (hypochromicity) and a small red shift Fig. 2. The change in the absorbance of the MLCT band with increasing amounts of CT-DNA was used to derive the intrinsic binding constants (K_b). The values of K_b derived for 1, 2, 3, and 4 complexes are $2.1 \pm 0.2 \times 10^5$, $1.9 \pm 0.2 \times 10^5$, $8.5 \pm 0.2 \times 10^4$ and $7.32 \pm 0.2 \times 10^4$ respectively. The different DNA-binding properties of complexes 1, 2, 3, and 4 are due to the different ancillary ligand. On going

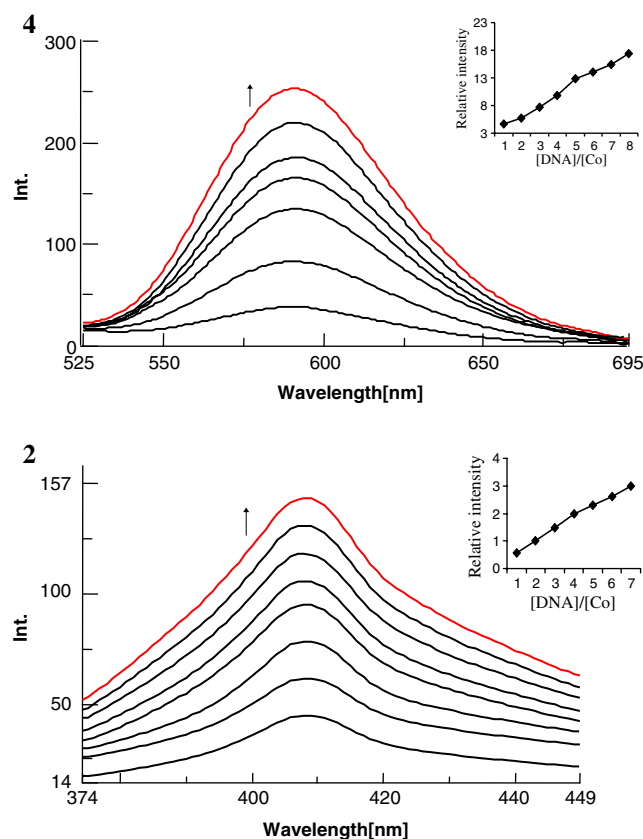
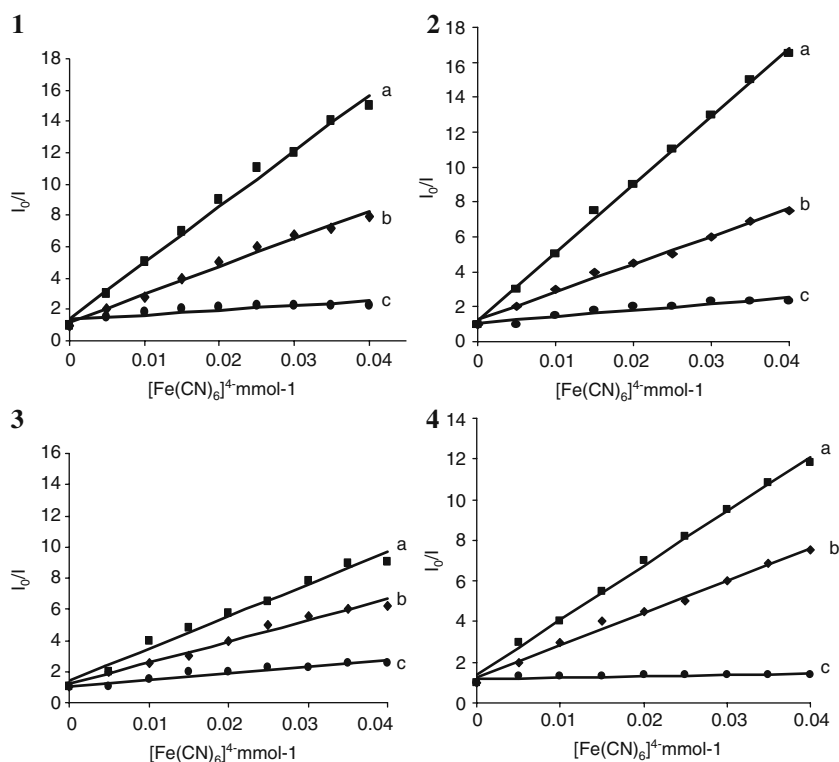


Fig. 3 Fluorescence emission spectra of complexes 2 and 4 in tris buffer in the presence of CT-DNA, where [cobalt or ruthenium]= 20 μM , [DNA]/Co=0, 5, 10, 15, 20 etc. The arrows indicate the intensity changes upon increasing concentration. Insert: plots of relative integrated emission intensity versus [DNA]/[Co]

Fig. 4 Emission quenching curves of complexes (1), (2), (3), and (4) in absence of DNA (a) presence of DNA (1:20) (b), excess of DNA (1:200 μ M) (c)



from bpy to phen, the plane area and hydrophobicity increases, and leading to a greater DNA-binding affinity for complex 1. The intrinsic binding constant K_b of four complexes with DNA is in the order $1 > 2 > 3 > 4$.

Fluorescence Quenching

Complexes 1, 2, 3 and 4 exhibit fluorescence in tris buffer at ambient temperature with λ_{\max} at 582, 408, 405 and 409 nm, addition of CT-DNA, the fluorescence emission intensities of 1, 2, 3 and 4 increased by a factor of 4.2, 3.2, 2.1 and 1.2 respectively. This indicates that the strong intercalation with DNA and the consequent restriction of mobility of the complexes at the binding site has the effect of enhancing, emission intensity Fig. 3. As per the procedures described [21], fluorescence quenching experiments were performed at ambient temperature with $K_4[Fe(CN)_6]^{4-}$ as the quenching agent. From the data for all complexes shown in Fig. 4, maximal quenching of fluorescence of DNA bound complex is seen with complex 1 and this effect decreases as one goes from complex 1 to complex 4.

Viscosity Measurements

Since Intercalation result in enhanced DNA viscosity [21, 22], viscosity of DNA in presence of complexes 1–4, have been determined as shown in Fig. 5. All complexes lead to

increased relative viscosity of DNA. Based on relative magnitude of viscosity binding affinity of complexes to DNA follows the order $1 > 2 > 3 > 4$ in agreement with the conclusion that these complexes intercalate between the base pairs of DNA.

Thermal Denaturation

To examine the effects of complex binding on thermal denaturation, all complexes were allowed to interact with DNA according to the conditions detailed and were heated

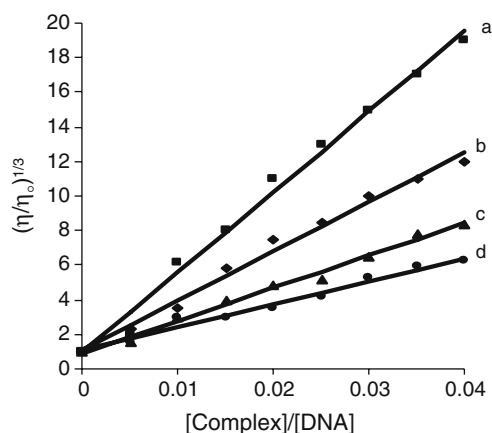


Fig. 5 Effect of increasing amount of complexes on the relative viscosities of CT DNA at 25 ± 0.1 °C complex -1 (a), complex-2 (b), complex -3 (c) and complex -4 (d)

from room temp up to 80 °C to obtain DNA melting curves from which T_m values were derived. Free un-complexed CT DNA used herein had a $T_m=60$ °C. T_m for each complex was determined as the difference between T_m of complex + DNA and T_m of DNA alone. On this basis T_m of complex increased by 4–7 °C, in the order 1>2>3>4 as shown by the data of Table 1. Thus the binding of complexes did enhance the stability of DNA and furthermore, strength of binding was greatest for complex 1, decreasing in the same order as indicated by other data of this study. (Table 1).

For the gel electrophoresis experiment, Supercoiled pBR322 DNA (0.1 μ g) was treated with the Ru(II) & Co (III) complexes in 50 mM Tris-HCl, 18 mM NaCl buffer, and the solution was then irradiated at room temperature with a UV lamp (365 nm, 10 W). The samples were analyzed by electrophoresis for 1.5 h at 80 V on a 0.8% agarose gel in TAE buffer. The gel was stained with 1 μ g/ml-1 ethidium bromide and photographed under UV light.

Photoactivated Cleavage of pBR322 DNA

There is substantial and continuing interest in DNA endonucleolytic cleavage reactions that are activated by metal ions [28, 29]. The cleavage reaction on plasmid DNA (pBR322 DNA) can be monitored by agarose gel electrophoresis. When circular plasmid DNA is subjected to electrophoresis, relatively fast migration will be observed for the intact supercoil form (Form I). If scission occurs on one strand (nicking), the supercoil will relax to generate a slower-moving open circular form (Form II). If both strands

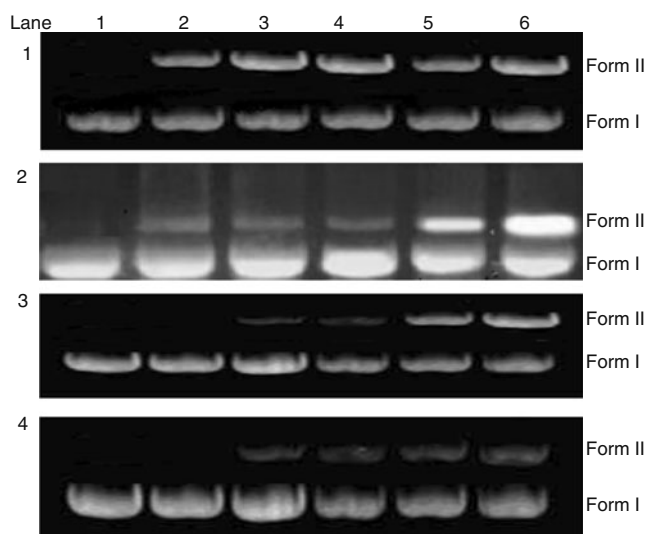


Fig. 6 Photocleavage of pBR 322 DNA, in absence and in the presence of complexes 1, 2, 3 and 4 light after 60 min irradiation at 365 nm. Lane 1 control plasmid DNA (untreated pBR 322), lanes 2 to 6 addition of complexes, in amounts of (0.01 M) 5, 10, 20, 30, 40 μ l of complex concentration

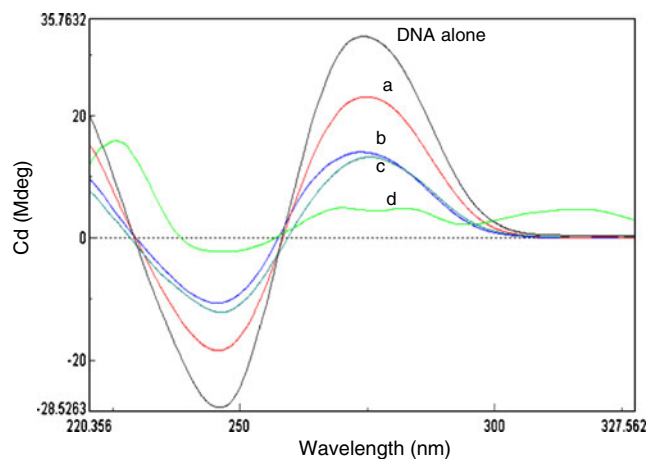


Fig. 7 Circular dichroism spectra of the dialysate of complexes 1 (a), 2 (b), 3 (c) and 4 (d) after 24 h dialysis against with CT DNA

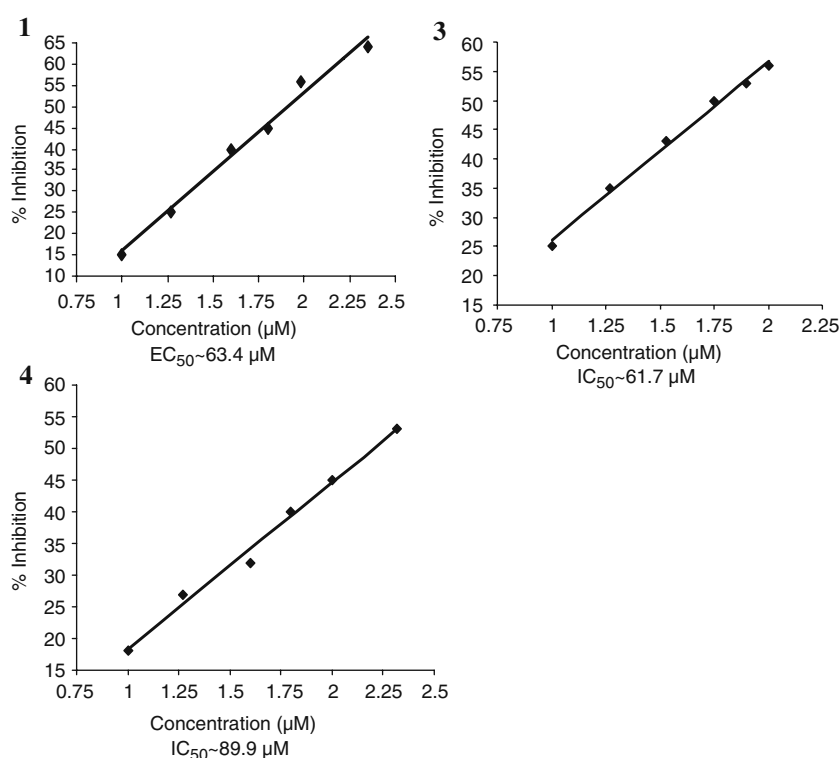
are cleaved, a linear form (Form III) that migrates between Form I and Form II will be generated [30]. The cleavage effect upon irradiation of the plasmid pBR322 DNA in the presence of different concentrations of complexes 1, 2, 3, and 4 have been tested and shown in Fig. 6 Lane 1 DNA alone, lanes 2–6 DNA + complexes with increasing concentration of complex. Form II increases of and, Form I decreases gradually as the concentration of complex increase. The results suggest concentration-dependent single-strand cleavage of supercoiled Form I to the nicked Form II. Under comparable experimental conditions, complex 1 exhibits more effective DNA cleavage activity than complexes 2, 3, and 4. The different cleaving efficiency may be ascribed to the different binding affinity of complexes to DNA.

Enantioselective Binding

A difference in biological activities between the enantiomers of an optically active metal complex has been noted in many examples such as toxicity and drug efficiency [31, 32]. In order to understand such affects better at the level of molecular interaction. It is of therefore important to examine enantiomeric effects on the DNA binding of a metal complex. According to the insertion model proposed by Barton and co-workers [22, 33], the Δ enantiomer of the complex, a right-handed propeller-like structure, will display a greater affinity than the Λ enantiomer with the right-handed CT-DNA helix, due to the appropriate steric matching. This discrimination can be observed via equilibrium dialysis experiments and provide strong evidence in support of intercalation.

The CD spectrum of CT DNA exhibits a positive band at 274 nm due to base stacking and a negative band at 243 nm due to the helicity of DNA. In the presence of complex an increase in the molar ellipticity values of the both positive and negative band of the CT DNA observed Fig. 7. It can

Fig. 8 Effects of complexes on the viability of HL-60 cells, following continuous incubation for 24 h, with increasing drug concentration (0.1–500 μM)



be concluded that the interaction of all the complexes towards CT-DNA follows the same order as the former experiments. Those significant changes indicate conformational changes and unwinding of DNA base pairs with destabilization of the DNA double helix, which is consistent with DNA intercalation mode suggested above.

Cytotoxicity Studies

Cell proliferation or viability was measured using the MTT [3-(4, 5-dimethylthiazol-2-yl)-2, 5-diphenyl tetrasodium bromide] assay [34]. Cells were seeded in each well containing 100 μl medium at a final density of 2×10^4 cells/well, in 96 well microtiter plates at identical conditions. After overnight incubation, the cells were treated with different concentrations of testing ligand complexes (20–100 $\mu\text{g}/\text{ml}$ in RPMI 1640 medium and filtered) in a final volume of 200 μl with five replicates each. After 24 h, 10 μl of MTT (5 mg/ml) was added to each well and the

plate was incubated at 37 $^{\circ}\text{C}$ in the dark for 4 h. The formazan crystals were solubilized in DMSO (100 $\mu\text{l}/\text{well}$) and the reduction of MTT was quantified by absorbance at 570 nm in a spectrophotometer (Spectra MAX Plus; Molecular Devices; supported by SOFT max PRO 3.0). Effects of test compounds on cell viability were calculated using cells treated with DMSO as control. The data were subjected to linear regression analysis and the regression lines were plotted for the best straight line fit Fig. 8. The IC_{50} (inhibition of cell viability) concentrations were calculated using the respective regression equation.

Observations

The cytotoxic effects of test complexes were investigated on human leukemia cell lines. After 24 h of treatment, the number of live cells were measured by MTT assay and IC_{50} values for each cell line were determined (Table 2). It is evident from Table 1 that HL-60 cells were sensitive to

Table 2 CD data for the interaction of CT DNA and Cytotoxic data of complex 1 to 4

Complexes	Positive peak	Negative peak	Cytotoxic activity of test complexes (IC_{50} values in μM)
DNA alone	274 243 nm	-246 nm	
1	273, 242 nm	-244 nm	63.4 μM
2	275, 243 nm	-246.1 nm	No activity
3	275.2 243 nm	-247 nm	61.7 μM
4	276.2 242 nm	-246.8 nm	89.9 μM

complex 1 and 3, with an IC_{50} value of 61.7 and 63.4 $\mu\text{g/ml}$, as compared with complex 4. Complex 2 did not show any activity against the HL-60 cells and the decreasing order of activity among the test complexes was in the order $1 > 3 > 4$ Fig. 8. The chemical structure of the mixed ligand complexes could be a factor for exhibiting differential anti-proliferative activities on the cancerous cell lines.

Conclusions

Four Ru(II) and Co(III) complexes of extended planar aromatic ligands have been isolated, characterized and their interaction with CT DNA examined. Absorption, Emission, thermal denaturation and viscosity experiments were performed and the result obtained suggests an intercalative mode of DNA binding for the four complexes. The planarity of the ligands plays an important role in dictating DNA binding affinity. Thus the complex 1 binds to DNA more strongly than remaining complexes binding, affinity follows the order $1 > 2 > 3 > 4$. The present study demonstrates that the ancillary ligands with hydrogen bonding potential support the intercalative interaction of ligands with extended aromatic rings and enhances the DNA binding affinity.

Acknowledgements We are grateful to G. Bhanuprakash reddy, Scientist-G, National Institute of Nutrition, Hyderabad for helping to record CD spectra and also grateful to DST New Delhi for financial support.

References

- Erkkila KE, Odem DT, Barton JK (1999) Recognition and reaction of Metallo intercalators with DNA. *Chem Rev* 99:2777–2796
- Metcalf C, Thomas JA (2003) Kinetically inert transition metal complexes that reversibly bind to DNA. *Chem Soc Rev* 32:215–224
- Maheswari PU, Palaniandavar M (2004) DNA binding and cleavage properties of certain tetrammine ruthenium(II) complexes of modified 1, 10-phenanthrolines—effect of hydrogen-bonding on DNA-binding affinity. *J Inorg Biochem* 98:219–230
- Deshpane MS, Kumbhar AA, Kumbhar AS (2007) Hydrolytic cleavage of DNA by a ruthenium(II) polypyridyl complex. *Inorg Chem* 46:5450–5452
- Yam VWW, Lo KKW, Cheung KK, Kong RYC (1997) Deoxyribonucleic acid binding and photocleavage studies of ruthenium(I) dipyrrophenazine complexes. *Dalton Trans* 12:2067–2072
- Liu XW, Li J, Li H, Zheng KC, Chao H, Ji LN (2005) Synthesis, characterization, DNA-binding and photocleavage of complexes $[\text{Ru}(\text{phen})_2(6\text{-OH-dppz})]^{2+}$ and $[\text{Ru}(\text{phen})_2(6\text{-NO}_2\text{-dppz})]$. *J Inorg Biochem* 99:2372–2380
- Metcalf C, Webb M, Thomas JA (2002) A facile synthetic route to bimetallic Re(I) Complexes containing two dppz DNA intercalating ligands. *Chem Commun* 18:2026–2027
- Mei W-J, Wang N, Liu Y-J, Ma Y-Z, Wang D-Y, Ling BX (2008) Studies on cytotoxic and DNA-binding properties of two ruthenium(II) complexes of a substituted phenanthroline ligand. *Transit Met Chem* 33:499–503
- Corral E, Hotze Anna CG, Den Dulk H, Leczkowski A, Rodger A, Hannon MJ, Reedijk J (2009) Ruthenium polypyridyl complexes and their modes of interaction with DNA: is there a correlation between these interactions and the antitumor activity of the compounds. *J Biol Inorg Chem* 14:439–448
- Kumar CV, Barton JK, Turro NJ (1985) Photo physics of ruthenium complexes bound to double helical DNA. *J Am Chem Soc* 107:5518–5523
- Henderson BW, Busch TM, Vaughan LA, Frawley NP, Babich D, Sosa TA, Zollo JD, Dee AS, Cooper MT, Bellnier DA, Greco WR, Osero AR (2000) Photofrin photodynamic therapy can significantly deplete or preserve oxygenation in human basal cell carcinomas during treatment, depending on fluence rate. *Cancer Res* 60:525–529
- Rajendiran V, Murli M, Suresh E, Palaniandavar M, Periasamy VS, Akbarsha MA (2008) Non-covalent DNA binding and cytotoxicity of certain mixed-ligand ruthenium (II) complexes of 2,2'-dipyridylamine and diimines. *Dalton Trans* 16:2157–2170
- Nagababu P, Satyanarayana S (2007) DNA binding and cleavage properties of certain ethylenediamine cobalt(III) complexes of modified 1, 10 phenanthrolines. *Polyhedron* 26:1686–1692
- Nagababu P, Latha JNL, Satyanarayana S (2006) DNA-binding studies of mixed-ligand (ethylenediamine) ruthenium(II) complexes. *Chem Biodivers* 3:1219–1229
- Shilpa M, Nagababu P, Satyanarayana S (2009) Studies on DNA-binding and plasmid-cleavage of cobalt (III) mixed ligand complexes. *Main Group Chem* 8(1):33–45
- Nagababu P, Shilpa M, Satyanarayana S, Naveena Lavanya Latha J, Karthikeyan KS, Rajesh M (2008) Interaction of cobalt (III) polypyridyl complexes containing asymmetric ligands with DNA. *Transit Met Chem* 33:1027–1033
- Yamada MT, Yoshimoto Y, Kuroda Y, Shimao S (1992) Synthesis and properties of diamino-substituted dipyrrodo [3, 2-a: 20, 30-c] phenazine. *J Bull Chem Soc Jpn* 65:1006–1011
- Marmur J (1961) A procedure for the isolation of DNA from microorganisms. *J Mol Biol* 3:208–218
- Reichmann ME, Rice SA, Thomas CA, Doty P (1954) A further examination of the molecular weight and size of desoxyribose nucleic acid. *J Am Chem Soc* 76:3047–3053
- Steck EA, Day AR (1943) Reactions of phenanthraquinone and retenequinone with aldehydes and ammonium acetate in acetic acid solution. *J Am Chem Soc* 65:452–456
- Chaires JB, Dattagupta N, Crothers DM (1982) Self association of daunomycin. *Biochemistry* 21:3927–3932
- Satyanarayana S, Dabrowiak JC, Chaires JB (1993) Tris (phenanthroline) ruthenium(II) enantiomer interactions with DNA: mode and specificity of binding. *Biochemistry* 32:2573–2584
- Barton JK, Danishefsky A, Raphael GJ (1984) Tris(phenanthroline) ruthenium (II): stereoselectivity in binding to DNA. *J Am Chem Soc* 106:2172–2176
- Ghosh BK, Chakravorty A (1989) Electrochemical studies of ruthenium compounds part I. Ligand oxidation levels. *Coord Chem Rev* 95:239
- Haga M-A (1983) Synthesis and protonation-deprotonation reactions of ruthenium(II) complexes containing 2, 2'-bibenzimidazole and related ligands. *Inorg Chim Acta* 75:29
- Baitalik S, Florke U, Nag K (1999) Synthesis, structure, redox activity and spectroscopic properties of ruthenium(II) complexes with 3, 5-bis (benzothiazol-2-yl)pyrazole, 3, 5-bis(benzimidazol-2-yl)pyrazole and 2,2'-bipyridine as co-ligands. *J Chem Soc Dalton Trans* 5:719–728
- Liu YJ, Wei XY, Wu FH, Mei WJ, He LX (2008) Interaction studies of DNA binding of ruthenium(II) mixed-ligand complexes: $[\text{Ru}(\text{phen})_2(\text{dtmi})]^{2+}$ and $[\text{Ru}(\text{phen})_2(\text{dtmi})]^{2+}$. *Spectrochimica Acta Part A* 70:171–176
- Johnston H, Katherine C, Glasgow H, PH T (1995) Electrochemical measurement of the solvent accessibility of nucleobases using

- electron transfer between DNA and metal complexes. *J Am Chem Soc* 117:8933–8938
29. Dallofo MH, Rodrigues B, Kuhn JB, Brown J, Wass G, Maegroves JP, Von Hoff DD, Rowrty EK (1998) A Phase I and pharmacological study of the glutamine antagonist acivicin with the amino acid solution amino synthesis in patients with advanced solid malignancies. *Clin Cancer Res* 4:2763–2770
 30. Barton JK, Raphael AL (1984) Photoactivated stereospecific cleavage of double-helical DNA by cobalt(III) complexes. *J Am Chem Soc* 106:2466–2468
 31. Wang AH-J (1992) Intercalative drug binding to DNA. *Curr Opin Struct Biol* 2:361–368
 32. Wang JG (1947) The degree of unwinding of the DNA helix by ethidium: I. Titration of twisted PM2 DNA molecules in alkaline cesium chloride density gradients. *J Mol Biol* 89:783–801
 33. Barton JK (1986) Metals and DNA: molecular left-handed complements. *Science* 233:727–734
 34. Mosmann T (1983) Rapid colorimetric assay for cellular growth and survival: application to proliferation and cytotoxicity assays. *J Immunol Methods* 65:55–63